Microporous and Mesoporous Materials 280 (2019) 105–115

Contents lists available at ScienceDirect

Microporous and Mesoporous Materials

journal homepage: www.elsevier.com/locate/micromeso

Landscape of AlPO-based structures and compositions in the database of zeolite structures

Xiaona Liu[a,b,1], Nana Yan[a,b,1], Lei Wang[a], Chao Ma[a], Peng Guo[a,*], Peng Tian[a], Guang Cao[c,**], Zhongmin Liu[a]

[a] National Engineering Laboratory for Methanol to Olefins, Dalian National Laboratory for Clean Energy, Dalian Institute of Chemical Physics, Chinese Academy of Sciences, Dalian, 116023, China
[b] University of Chinese Academy of Sciences, Beijing, 100049, China
[c] Corporate Strategic Research, ExxonMobil Research and Engineering Co., 1545 Route 22 East, Annandale, NJ, 08801, USA

ARTICLE INFO

Dedication to Prof. Wieslaw J. Roth on the occasion of his 65th birthday.

Keywords:
AlPO-based molecular sieves
Layered structures
ADOR method

ABSTRACT

Aluminophosphate-based (AlPO-based) molecular sieves (MSs), especially silicoaluminophosphates (SAPO), have found increasing commercial use in adsorptive and catalytic applications. Although there are 245 framework type codes (FTCs) deposited in the zeolite database, only 74 of which are considered as AlPO-based MSs. In this article, firstly, the landscape of three-dimensional (3D) AlPO-based MSs in the zeolite database, including SAPOs, AlPOs, and metalloaluminophosphates (MeAPOs), is summarized and categorized. Secondly, inspired by the systematic investigations of two-dimensional (2D) layered silicates from Prof. Wieslaw J. Roth, the structural transformations of 2D SAPO or AlPO layered materials into 3D zeotype frameworks are elucidated. Last but not least, the potential application of the ADOR method is introduced to the SAPO material. This approach has been widely used for synthesizing new zeolites through a series of steps involving an **a**ssembly, **d**isassembly, **o**rganization, **r**eorganization on the parent germanosilicates. The open question regarding the application of this synthetic method on the unique SAPO ECR-40 is discussed.

1. Introduction

Aluminophosphates (AlPOs), the isoelctronic analogues of all-silica zeolites, were first reported by Wilson et al. at Union Carbide Corporation in 1982 [1]. The basic building units TO_4 (tetrahedral atoms, T = Al and P) are alternately distributed, generating a neutral three-dimensional (3D) framework with well-defined channels or cavities of the size of small molecules. Subsequently it was discovered that substitutions of Si for P, or metals for Al, in the AlPO frameworks led to silicoaluminophosphates (SAPOs) and metalloaluminophosphates (MeAPOs), respectively. These substitutions effectively introduce Brønsted acid into the AlPO-based molecular sieves (MSs). Based on the pore openings delimited by the T atoms, AlPO-based MSs can be categorized into small pore (8 T), medium pore (10 T), large pore (12 T), and extra-large pore (> 12 T). AlPO-based MSs, especially SAPOs, have attracted increasing attention for their applications in catalytic and adsorptive processes, such as the methanol-to-olefins (MTO) reaction [2], the selective catalytic reduction (SCR) of NO_X [3], the isomerization of wax [4], the disproportionation of toluene [5], and the separation of CO_2 [6].

Up till the drafting of this manuscript, there are 245 zeolites or zeolite-related porous materials that have been approved and assigned three-letter framework type codes (FTCs) by the International Zeolite Association's Structure Commission [7,8]. These framework type codes form a structural landscape that is independent of chemical compositions. For example, the aluminosilicate Rho and SAPO DNL-6 (DNL stands for Dalian National Lab) have different chemical compositions but share the same **RHO** FTC. The basic structural information in this zeolite database such as unit cell parameters, space group, atomic coordinates, channel systems, etc. can be searchable. Moreover, in our recent work, we have summarized the intrinsic structural information on zeolites including characteristic unit cell dimensions, butterfly layers, zeolites containing the same building layers, ABC-6 zeolite family, and the embedded isoreticular **RHO** family [8].

In this article, we attempt to first summarize and categorize the AlPO-based MSs deposited in this database. In this case, a new map of

* Corresponding author.
** Corresponding author.
E-mail addresses: pguo@dicp.ac.cn (P. Guo), guang.cao@exxonmobil.com (G. Cao).
[1] These authors contributed equally.

https://doi.org/10.1016/j.micromeso.2019.01.047
Received 27 November 2018; Received in revised form 17 January 2019; Accepted 28 January 2019
Available online 31 January 2019
1387-1811/

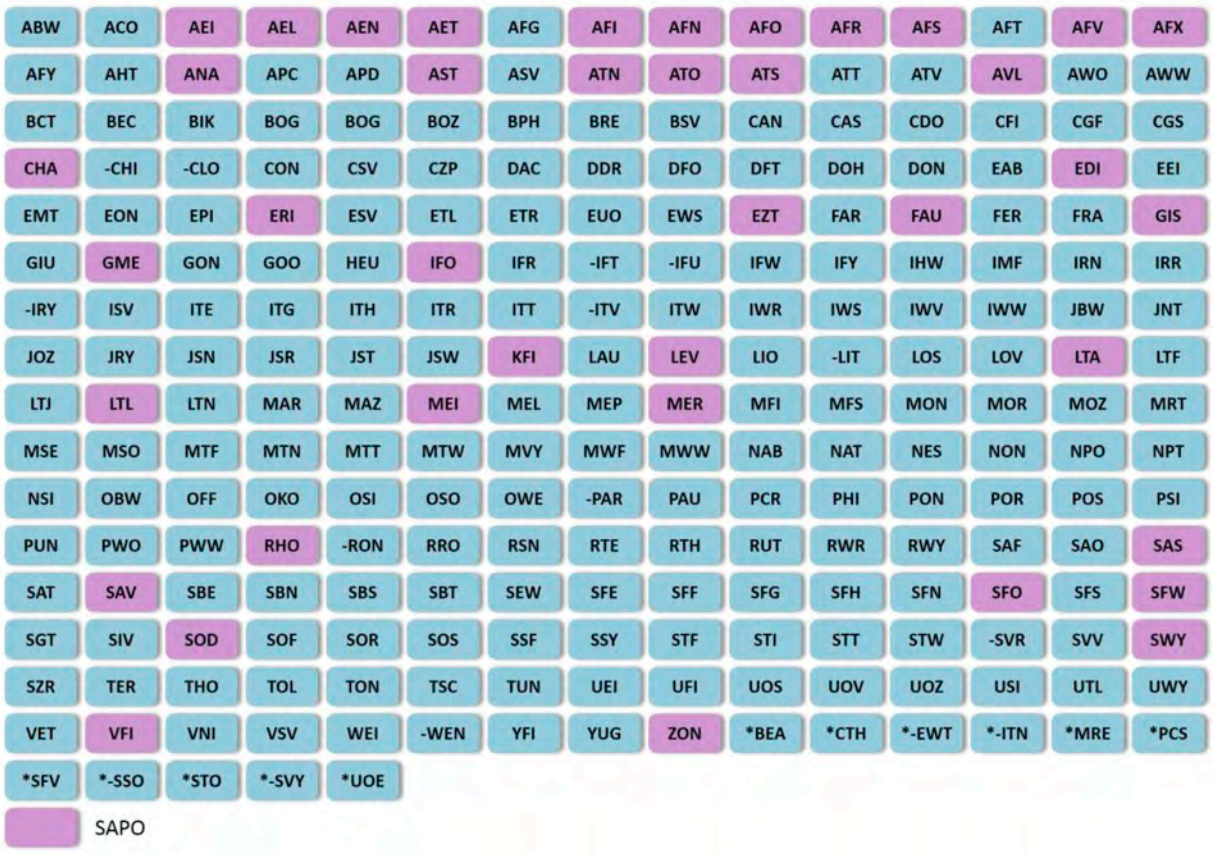

Fig. 1. The landscape of SAPO MSs in the zeolite database.

Table 1
Novel AlPO-based MSs with new topologies.

FTC	Material Name	Chemical Composition	Channel System	Year of code assigned	References
AFV	SAPO-57, AlPO-57, MeAPO-57	SAPO, AlPO, MeAPO	2D 8 × 8	2013	[11]
AVL	SAPO-59, AlPO-59, MeAPO-59	SAPO, AlPO, MeAPO	2D 8 × 8	2013	[11]
IFO	ITQ-51	SAPO, AlPO	1D 16	2013	[12]
JNT	JU-92-300	MeAPO	2D 8 × 8	2015	[13]
JRY	CoAPO-CJ40	MeAPO	1D 10	2009	[14]
JSN	CoAPO-CJ69	MeAPO	2D 8 × 8	2012	[15]
JSW	CoAPO-CJ62	MeAPO	1D 8	2012	[16]
POR	PST-14	AlPO	3D 8 × 8 × 8	2018	[17]
PSI	PST-6	AlPO	1D 10|8	2015	[18]
SAF	STA-15	AlPO	1D 12	2010	[19]
SWY	STA-20	SAPO	3D 8 × 8 × 8	2017	[20]

FTCs has been drawn for identifying the landscape of AlPO-based MSs in the database, which will be complementary to the current FTC map. In this section, several AlPO-based MSs with 3D frameworks will be further highlighted because of their unique structural features, synthetic approach, or chemical compositions. We will then focus on the transformation of two-dimensional (2D) AlPO-based layered structures to three-dimensional (3D) zeotype frameworks. Compared with the extensively-investigated 2D to 3D transformations in silicate-based materials, to which Prof. Wieslaw J. Roth has made great contributions [9], reports regarding AlPO-based structures are still rare. Two (silico) aluminophosphates layered structures and their structural transformations from 2D structures to 3D zeotype frameworks will be reviewed. Finally, we put forth a question – Can the ADOR approach, pioneered by Profs. Wieslaw J. Roth, Jiři Čejka, and Russel Morris, be applied to AlPO-based materials? The concept of ADOR approach refers to a novel strategy for synthesizing new zeolites through an **a**ssembly, **d**isassembly, **o**rganization, and **r**eassembly of the parent germanosilicates [10]. Hence, this ADOR approach is expected to be utilized in the SAPO materials. We propose a potential SAPO MS candidate, ECR-40 (**MEI**), for the further discussion.

2. The landscape of 3D AlPO-based MSs

We have identified 40 SAPO MSs (Fig. 1), 44 AlPO MSs (Fig. S1), and 51 MeAPO MSs (Fig. S2) with a thorough literature search. To the best of our knowledge, there have been no reports on the successful synthesis of the SAPO form of 34 AlPO-based MS listed in Fig. S3, *i. e*, they have been prepared in the AlPO or MeAPO form. In the last decade, 11 new FTCs unique to AlPO-based MSs with fascinating structures have been reported (Table 1), while the chemical compositions of another 10 known FTCs have been extended to (silico)aluminophosphates, as listed in Table 2. Hence, in this section, several new SAPO or AlPO frameworks and known

Table 2
Known frameworks with new (silico)aluminophosphate chemical compositions.

FTC	Material Name	Chemical Composition		Channels	References*
		New	before		
AFN	SAPO-14	SAPO	AlPO and MeAPO	3D 8 × 8 × 8	[21]
-CLO	DNL-1	AlPO	gallophosphate	3D 20*20*20|8*8*8	[22]
EDI	K-SAPO-EDI	SAPO	aluminosilicate and MeAPO	3D 8 × 8 × 8	[23]
GME	STA-19	SAPO	aluminosilicate	3D 12 × 8 × 8	[24]
KFI	STA-14	SAPO	aluminosilicate	3D 8 × 8 × 8	[25]
LTL	SAPO-LTL	SAPO	aluminosilicate and AlPO	1D 12	[26]
MER	K-SAPO-MER	SAPO	aluminosilicate and MeAPO	3D 8 × 8 × 8	[23]
RHO	DNL-6	SAPO	aluminosilicate and MeAPO	3D 8 × 8 × 8	[27]
SAV	STA-7	SAPO	MeAPO	3D 8 × 8 × 8	[25]
SFW	STA-18	SAPO	aluminosilicate	3D 8 × 8 × 8	[24]

*References refer to the recently-reported structures with known frameworks in (silico)aluminophosphate chemical compositions.

frameworks with (silico)aluminophosphate chemical compositions will be highlighted as follows.

2.1. ITQ-51 (IFO)

ITQ-51 is the first thermally stable SAPO MS with 16-ring extra-large pores (Fig. 2a), which was synthesized using 1, 8-bis (dimethylamino) naphthalene (DMAN) as the organic structure directing agents (OSDA) [12]. Its structure was solved by rotation electron diffraction (RED) method and further refined against power X-ray diffraction (PXRD). The framework is composed of *lau* chains (Fig. 2b) and unique helical four-ring chains (along the *b*-axis) (Fig. 2c). Each *lau* chain links with four helical four-ring chains, while each helical four-ring chain connects with two *lau* chains, creating 1D 16-ring channels along the *b*-axis (Fig. 2a). The location and π−π interaction of OSDAs were identified through Rietveld Refinement based on the as-made sample [28]. If helical four-ring chains in the **IFO** framework are replaced by *lau* chains, the **ATO** framework (type material: AlPO-31) (Fig. 2d) will be constructed. Similarity, a hypothetical 1D 18-ring zeolite has been predicted when the *lau* chains in the **IFO** framework are substituted by helical four-ring chains (Fig. 2e).

2.2. PST-6 (PSI)

From the structural point of view, PST-6 (a novel 1D medium pore AlPO MS) is the most complex zeolite solved up to now (Fig. 3a), which has 36 distinct T atoms and 72 O atoms in the asymmetric unit [18]. It was obtained by the calcination of PST-5, which was synthesized using simple organic amine diethylamines as OSDAs. PXRD combined with RED and computer modeling have been applied to the structure determination of PST-6. There are single crankshaft chains (Fig. 3b) and narsarsukite chains (*nsc*) (Fig. 3c) running along the *a*-axis.

2.3. STA-20 (SWY)

STA-20 is a novel 3D small pore SAPO MS, which is a potential candidate for catalytic processes such as SCR of NO_X (Fig. 4a) [20]. Both hexamethylene bisdiazabicyclooctane (diDABCO-C6) and trimethylamine (TrMA) were used as OSDAs. It first appeared as an impurity of synthesis STA-18 (described latter). Through optimizing synthetic conditions such as the Si content, the TrMA/diDABCO-C6 ratio, the crystallization time, and temperature, the pure STA-20 was successfully obtained. Its initial structure model was adopted from the hypothetical zeolite database, which was further confirmed by high-resolution transmission electron microscopy (HRTEM) and Rietveld refinement. In 2017, STA-20 was assigned a three-letter code as **SWY**. It

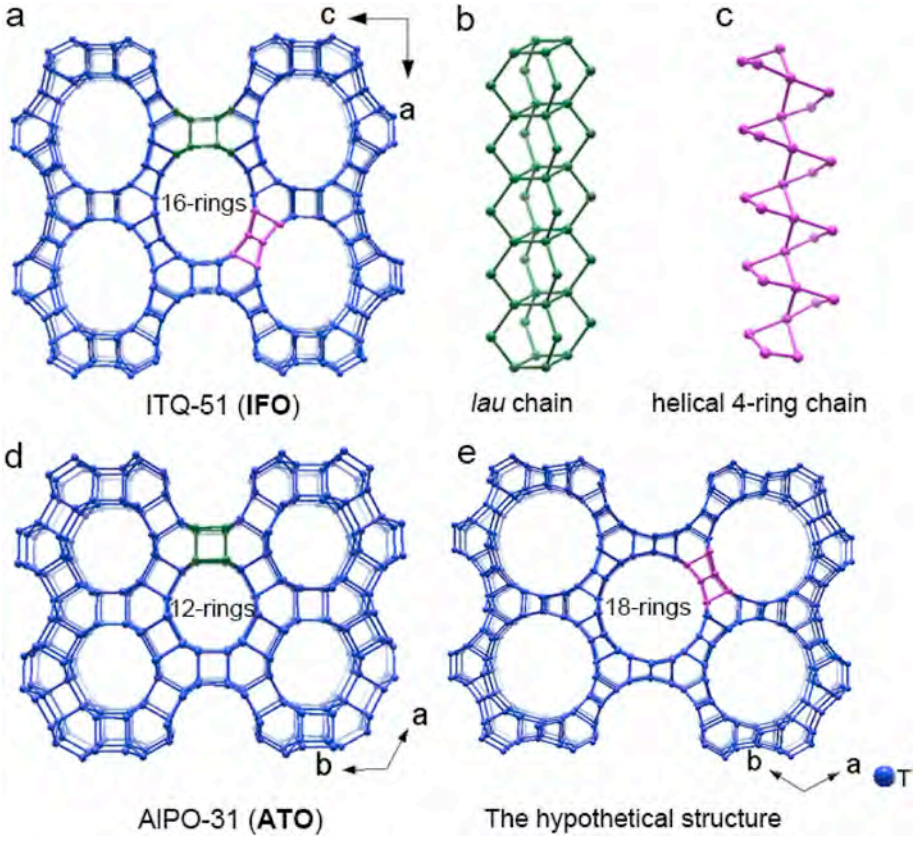

Fig. 2. Structural models of ITQ-51 (**IFO**) (a), AlPO-31 (**ATO**) (d), and a hypothetical structure with a 1D 18-ring channel system (e). The *lau* chain (b) and helical four-ring chain (c) along the *b*-axis are highlighted in green and pink, respectively. For clarity, O atoms are omitted. (For interpretation of the references to colour in this figure legend, the reader is referred to the Web version of this article.)

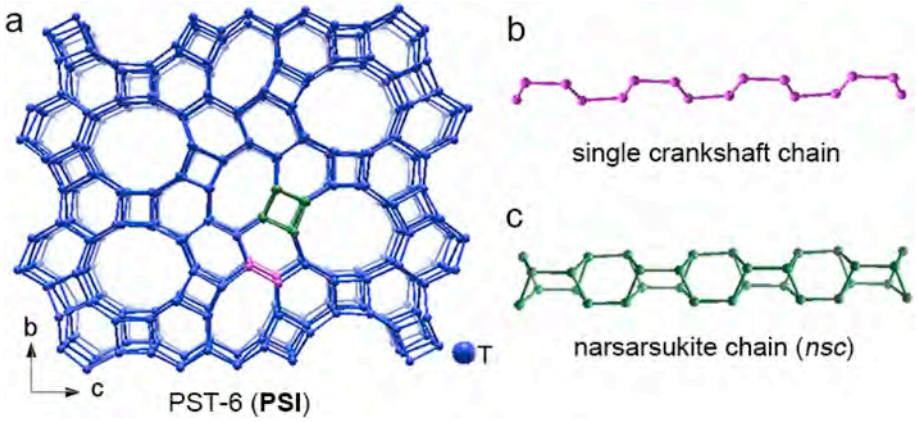

Fig. 3. 3D Structural model of PST-6 (**PSI**) (a). The single crankshaft chain (b) and narsarsukite chain (*nsc*) (c) running along the *a*-axis are highlighted in pink and green, respectively. For clarity, O atoms are omitted. (For interpretation of the references to colour in this figure legend, the reader is referred to the Web version of this article.)

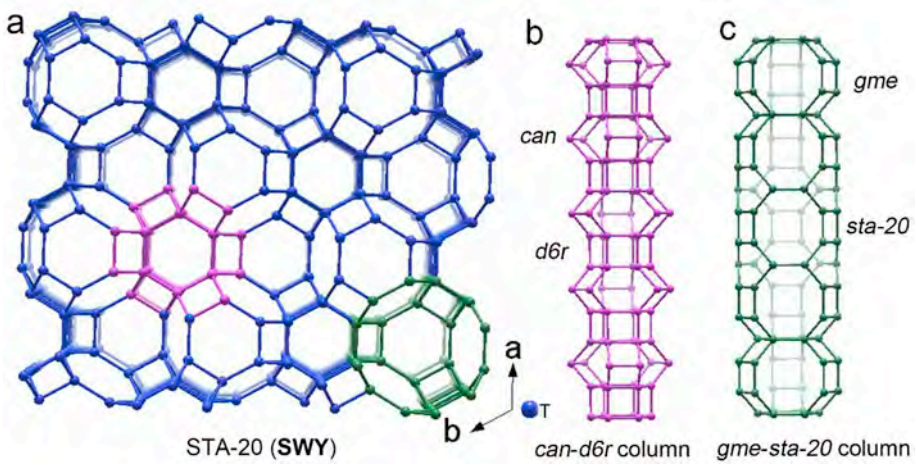

Fig. 4. Structure of STA-20 (**SWY**) (a). The *can-d6r* column (b) and *gme-sta*-20 column (c) running along the *c*-axis are highlighted in pink and green, respectively. For clarity, O atoms are omitted. (For interpretation of the references to colour in this figure legend, the reader is referred to the Web version of this article.)

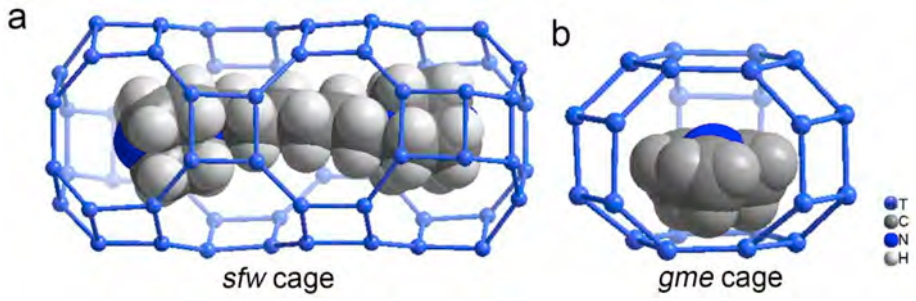

Fig. 5. DiDABCO-C6 (a) and TrMA (b) are distributed in *sfw* and *gme* cages in the as-made STA-18, respectively. For clarity, O atoms are omitted.

consists of *can-d6r* columns (alternating *can* and *d6r* composite building units (CBUs)) and *gme-sta*-20 (alternating *gme* and *sta*-20 cages) columns running along the *c*-axis, as shown in Fig. 4b and c, respectively. The final Rietveld refinement demonstrates that the TrMA and diDABCO are mainly distributed in the *gme* and *sta*-20 cages, respectively.

2.4. STA-18 (*SFW*)

In 2016, Paul A. Wright's group developed a retrosynthetic co-templating method for the designed synthesis of *gme*-cage-based SAPO MSs [24]. They search for suitable OSDAs for stabilizing specifically isolated cages (based on the AlPO framework) with the aid of the molecular modeling approach. Using this method, the SAPO-form STA-18 (**SFW**) was successfully synthesized. Moreover, Rietveld refinement result shows that diDABCO-C6 and TrMA locate in *sfw* and *gme* cages (Fig. 5), respectively. This result is consistent with the result of molecular modeling. It is worth noting that SSZ-52 [29], which is the **SFW**-type aluminosilicate synthesized by Chevron, has **CHA**-type stacking faults, while STA-18 is a stacking-fault-free SAPO material. Moreover, the SAPO **GME**-type STA-19 was also synthesized using the identical method.

2.5. DNL-6 (*RHO*)

The targeted synthesis of conventional zeolites and SAPO MSs is attractive for zeolite scientists. As mentioned in the last paragraph, a retrosynthetic co-templating method was developed for synthesizing

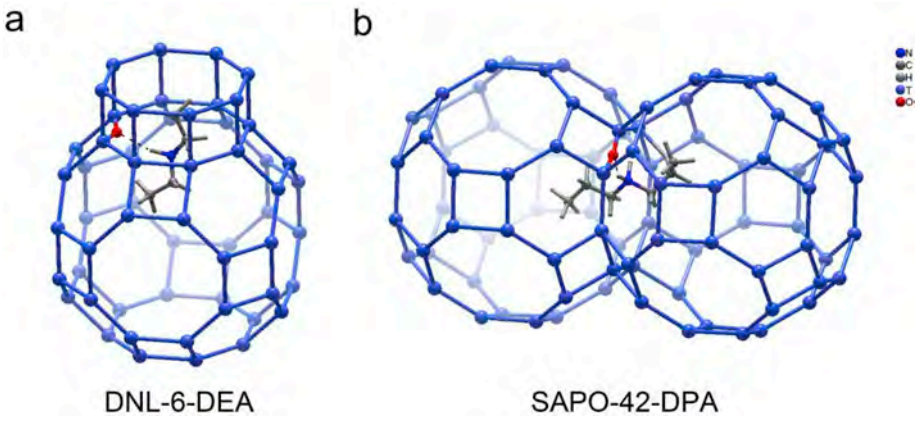

Fig. 6. Locations of OSDAs and host–guest interactions in the as-made DNL-6-DEA (a) and SAPO-42-DPA (b), respectively. For clarity, the O atoms are omitted except for the one which generates the hydrogen bonding interaction with the N atom of OSDA.

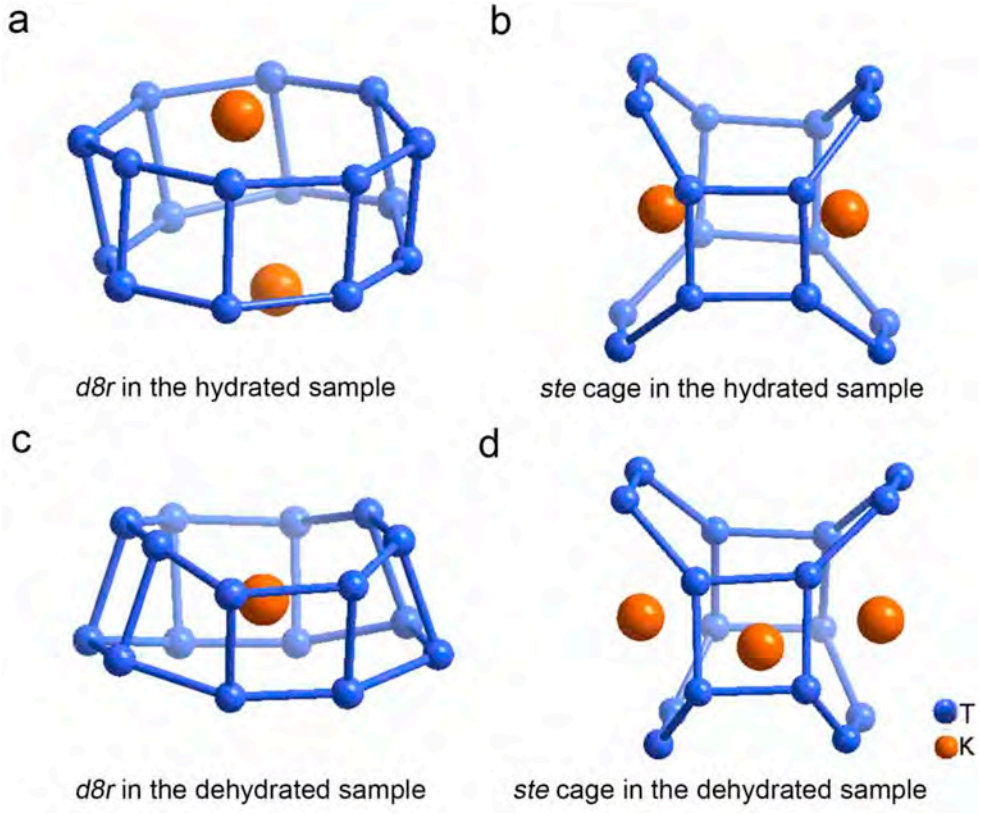

Fig. 7. Distributions of K^+ ions in the hydrated sample (a and b) and dehydrated sample (c and d). For clarity, O atoms are omitted.

gem-cage-based SAPO materials. Recently, our group has developed an alternative approach called **RSS** (**R**efine, **S**ummarize, and **S**earch) to facilitate the targeted synthesis of specific MSs of known frameworks [30]. This approach has been successfully applied to the targeted synthesis of SAPO **RHO**-type DNL-6, which was initially synthesized by using N, N′- dimethylethylenediamine (DEA) as the OSDA in our lab [27]. Based on the structural role of DEA and the host-guest interaction revealed from refinement results (Fig. 6a), we search for the possible OSDAs among commercialized ones with similar structural features for DNL-6. Through this **RSS** method, we identified another fourteen templates for SAPO **RHO**-type DNL-6. All the OSDAs stretch across *d8rs* and *lta* cages. Moreover, this method can also be applied to other cage-based SAPO materials such as SAPO-42 (**LTA**) as shown in Fig. 6b.

2.6. K-SAPO-MER (*MER*)

In most cases, only OSDA was utilized in the synthesis of AlPO-based MSs. Recently, Prof. Hong's group has synthesized a series of SAPO MSs using inorganic cations as SDAs solely [23]. This highly basic gel is unprecedented in SAPO, but common in the synthesis of low silica-to-alumina ratio aluminosilicates. More interestingly, the number of K^+ ions in the channels of SAPO **MER**-type MS can be tunable through adjusting the Si content in the synthesis gel. The location of K^+ ions has been investigated by Rietveld refinement. Take K-SAPO-**MER** (2) for example. The distribution of K^+ is different in hydrated and dehydrated samples. In the hydrated sample, K^+ ions locate on the 8-ring pore openings of *d8r* (Fig. 7a) and *ste* cages (Fig. 7b). It is of in-

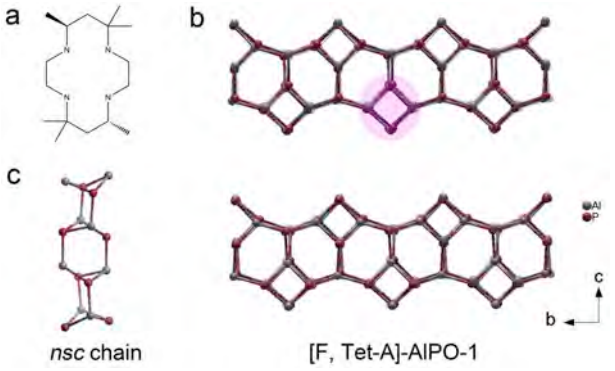

Fig. 8. (a) Tet-A (*meso*-5,7,7,12,14,14-hexamethyl-1,4,8,11-tetraazacyclotetradecane) used as the OSDA for synthesizing [F, Tet-A]-AlPO-1. (b) The layered structure of [F, Tet-A]-AlPO-1 without OSDA between the AlPO *afo* layers. The *nsc* chain within the *afo* layer has been highlighted in pink. (c) The *nsc* chain along the *a*-axis. (For interpretation of the references to colour in this figure legend, the reader is referred to the Web version of this article.)

terest to note that some K^+ ions move into the middle of *d8r* (Fig. 7c) and *ste* cages (Fig. 7d) in the dehydrated sample. Unfortunately, the structure of SAPO-**MER** will collapse after NH_4^+ exchange followed by the calcination. Using the identical synthetic strategy, they also synthesized SAPO MSs with **EDI**, **GIS**, and **ANA** frameworks.

3. Structural transformation of 2D layered (silico) aluminophosphates into 3D zeotype framework

Prof. Wieslaw J. Roth, who is one of the pioneers leading the field of 2D layered zeolites, has made great contributions to the development of this field. In this section, we would like to extend this concept to the 2D zeolitic (silico)aluminophosphate materials. The recent investigations regarding the 2D zeolitic (silico)aluminophosphate materials and their structural transformations to 3D frameworks will be highlighted. To the best of our knowledge, there are only two cases belonging to the current topic. The first reported case, [F, Tet-A]-AlPO-1, was synthesized using a bulk macrocycle polyamine Tet-A as the OSDA (Fig. 8a) [31]. Its structure was solved by the conventional single crystal X-ray diffraction (SCXRD) and possesses a 2D zeolitic AlPO material (Fig. 8b). The narsarsukite chain (*nsc*) as shown in Fig. 8c along the *a*-axis in the layer (denoted as *afo* layer) is identified. The OSDAs are occluded between the *afo* layers. The 3D **AFO**-type AlPO material will be obtained by assembling the AlPO *afo* layers as illustrated in Fig. 9 [32]. The *c*-dimension of its unit cell parameters (8.359 Å) indicates the presence of *nsc,* which has been summarized in our database-mining work [8].

If *afo* layers are considered as building units without considering the alternation of Al and P, the 3D **AFO** framework can be constructed by assembling *afo* layers through an inversion center. Our previous work has elucidated the structural correlations of a series of 3D zeolite frameworks containing the identical layers but assembled by distinct symmetries (an inversion center or a mirror symmetry) [8]. Inspired by these preliminary results, a hypothetic structure possessing the identical AlPO *afo* layers can be generated through another assembling process as illustrated in Fig. 10. Similarly, if the ordered distribution of Al and P is not taken into account, the hypothetical structure can be built by applying a mirror symmetry to *afo* layers. The crystallographic details for AlPO-form and idealized pure-silica hypothetical structures are listed in Tables S1, S2, S3, and S4. As demonstrated in Fig. 10g and h, the new structure has a 2D 10x8-ring channel system between *afo* layers. However, 8-ring pore opening along the *a*-axis is elliptical as illustrated in Fig. 10g. As a contrast, the 3D **AFO** framework (the case of inversion center symmetry) only possesses 1D 10-ring straight channels between *afo* layers.

The other example is recently reported 2D zeolitic layered (silico) aluminophosphate EMM-9 (Fig. 11a), which can transform into 3D

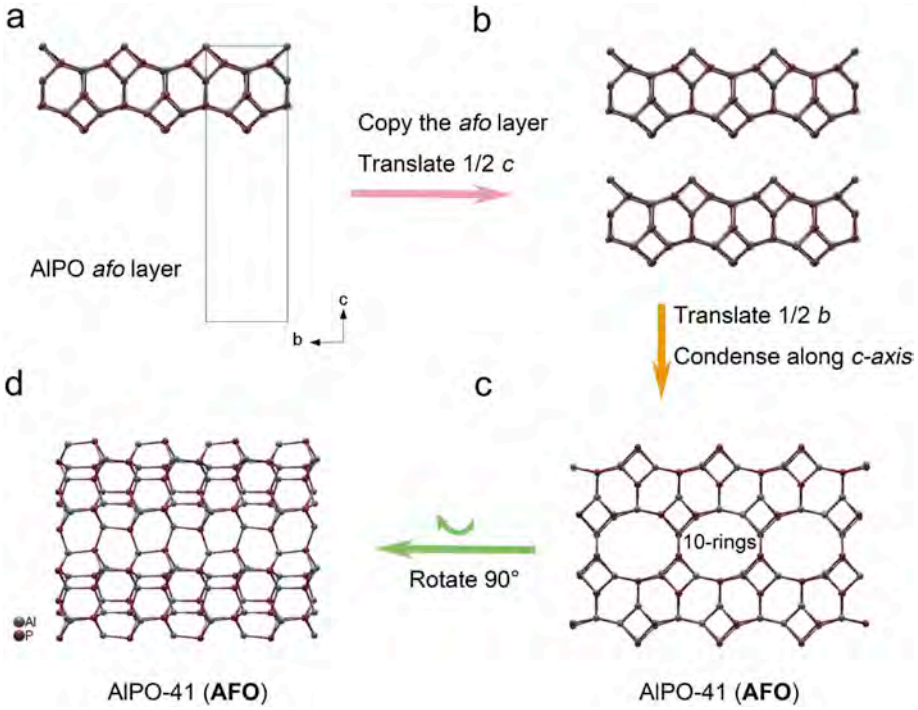

Fig. 9. The 3D **AFO** structure (AlPO-41) assembled from 2D AlPO *afo* layers. The identical *afo* layer is copied and translated by 1/2 *c* (a and b). This layer is translated by 1/2 *b* with respect to one another and then condensed along the *c*-axis to form the 3D **AFO** framework (c and d).

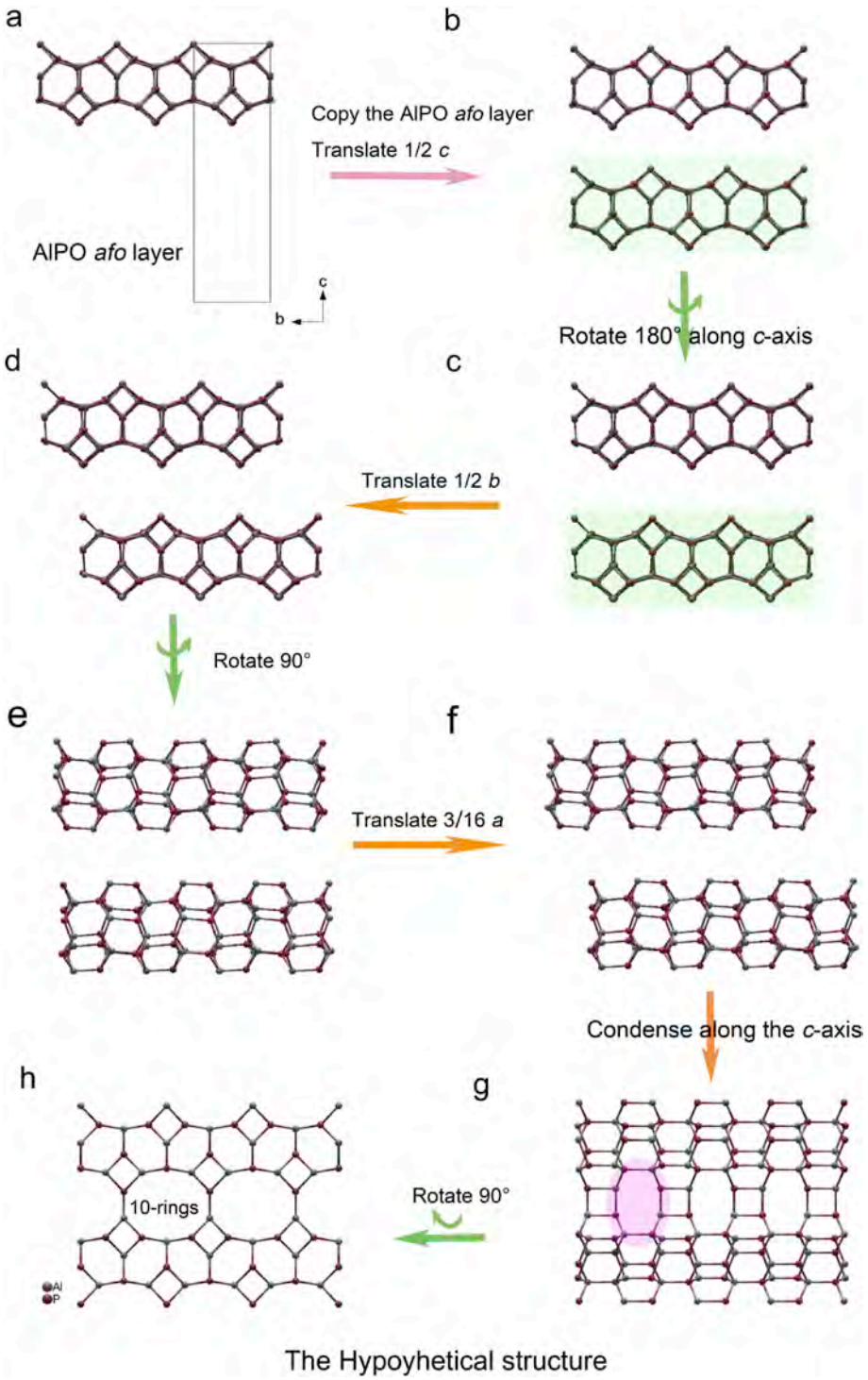

Fig. 10. The 3D hypothetical structure constructed by assembling AlPO *afo* layers. The identical *afo* layer (a) is copied and translated by 1/2 *c* (b), highlighted in green. This layer is rotated 180° along *c*-axis (c) with respect to one another, translated by 1/2 *b*, and 3/16 *a* (d, e, and f). Then the layers are condensed along the *c*-axis to form a 3D framework (g and h). The elliptical 8-rings is highlighted in Fig. 10g. (For interpretation of the references to colour in this figure legend, the reader is referred to the Web version of this article.)

EMM-8 (**SFO**) after the calcination [33]. EMM-8 and SSZ-51 share the same **SFO** FTC [34,35]. Both of them were synthesized using 4-(dimethylamino)pyridine (DMAP) as the OSDA. Moreover, EMM-9 was also obtained in the similar synthesis system but with a higher F^- content in the gel composition. The structure of AlPO-form EMM-9 was solved from RED data using direct method. EMM-9 is built up from inorganic AlPO-based layers (denoted as *sfo* layer) and DMAPs are located between the *sfo* layers. Furthermore, $\pi-\pi$ interactions between the DMAP cations and the host-guest interactions have been identified through Rietveld refinement against synchrotron PXRD data. The *sfo* layer consists of *sti* CBUs, which are described as the double 4-rings with one edge disconnected. They are connected by the "head-to-tail" arrangement, forming a 1D *sti* chain along the *a*-axis (Fig. 11b). The *sti* chain is further linked with the adjacent antiparallel one through 4-

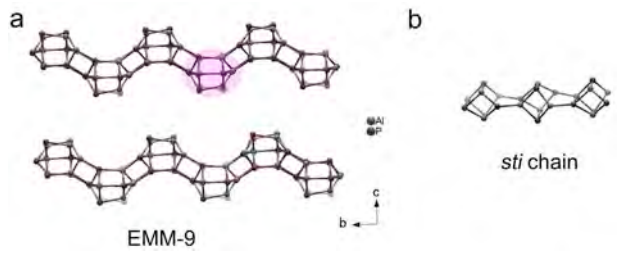

Fig. 11. (a) The structural model of the 2D layered EMM-9 without OSDAs between AlPO *sfo* layers. The *sti* chain building unit has been highlighted in pink. (b) The *sti* chain assembled in the "head-to-tail" mode along the *a*-axis. (For interpretation of the references to colour in this figure legend, the reader is referred to the Web version of this article.)

rings to form undulating *sfo* layers. After the careful calcination, the 2D layered EMM-9 transforms into 3D EMM-8. Similar to the first case, the translation of adjacent layers (by 1/3 *a* and 1/2 *b*) are required before the *sfo* layers condense along the *c*-axis as explained in Fig. 12.

It is worth pointing that the **AFR** framework has the same building unit *sfo* layer [36,37]. The **AFR** framework can be generated by assembling *sfo* layers as shown Fig. 13. Without considering the alternation of Al and P, the *sfo* layers in the **AFR** framework are connected through the mirror symmetry, while the inversion center symmetry is applied to the further connection of *sfo* layers in the **SFO** framework. Both structures have 2D 12x8-ring channel systems between *sfo* layers (Fig. 12e, f, 13e, and 13f).

4. Can the ADOR approach be applied to AlPO-based materials?

The ADOR (assembly, disassembly, organization, and reassembly) synthetic method is a top-down strategy regarding targeted synthesis of specific zeolites with desirable pore openings [10,38]. This approach was first demonstrated in the germanosilicate IM-12 (**UTL**) with a 14x12-ring channel system [10]. IM-12 is usually synthesized by using (6R, 10S)-6,10-dimethyl-5-azoniaspiro [4,5] decane hydroxide as the OSDA [39]. The first step, the "assembly", is the crystallization of a zeolite from the starting materials. The "disassembly" step takes advantage of the weakness of the Ge-O bonds that are preferentially distributed in the double 4-rings (*d4rs*). Through appropriate post treatments, the Ge-rich *d4rs* is removed and then the parent 3D framework is transformed into a 2D layered structure (disassembly). In the "organization" step, new linking units or SDAs will be incorporated into the interlamellar space between the layers, setting up for the final "reassembly" of layers by forming new interlamellar bonds that leads to new and fully connected zeolites with targeted pore sizes. Utilizing this novel approach, IPC-2 (**OKO**), IPC-4 (**PCR**), IPC-9, and IPC-10 have been successfully prepared [10,40].

An interesting question may be asked about whether the ADOR approach can be applied to AlPO-based materials which, if successful, would lead to novel materials. The [F, Tet-A]-AlPO-1/AlPO-41 and EMM-9/EMM-8 examples above show a partial answer to this question.

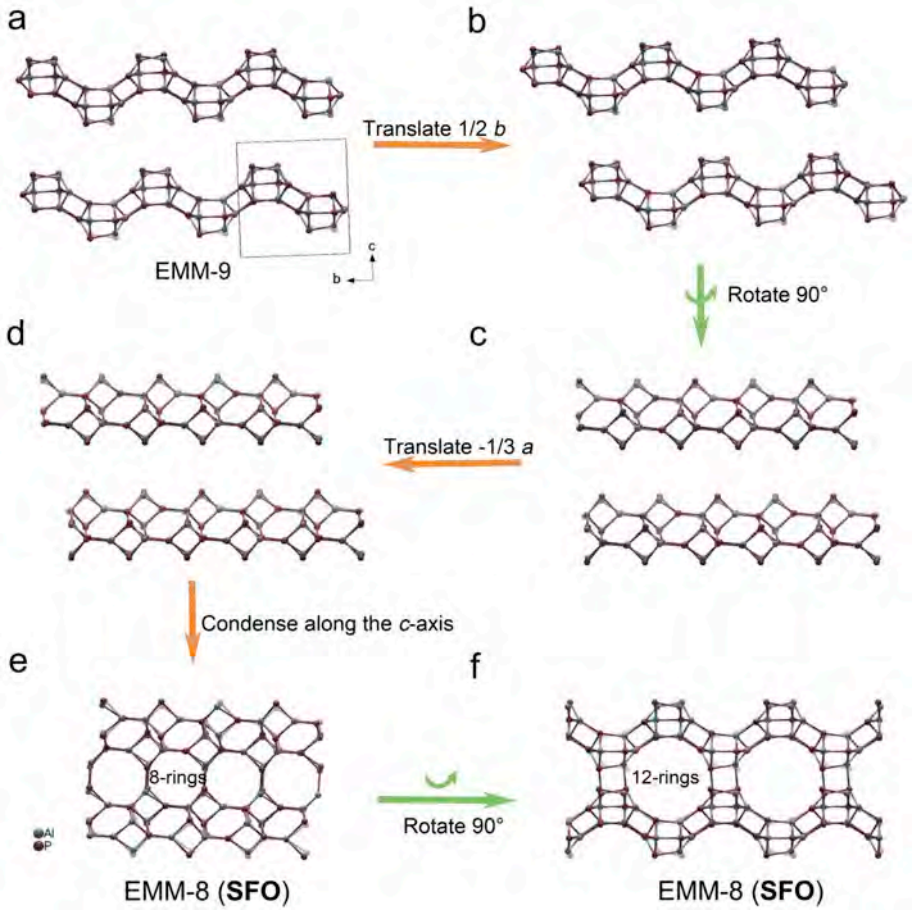

Fig. 12. The structural transformation of the 2D layered EMM-9 into the 3D **SFO** framework. The AlPO *sfo* layer (a) is translated by 1/2 *b* with respect to the adjacent one (b and c) and then translated by −1/3 *a* (d). The layers are condensed along the *c*-axis to form the 3D **SFO** framework (e and f).

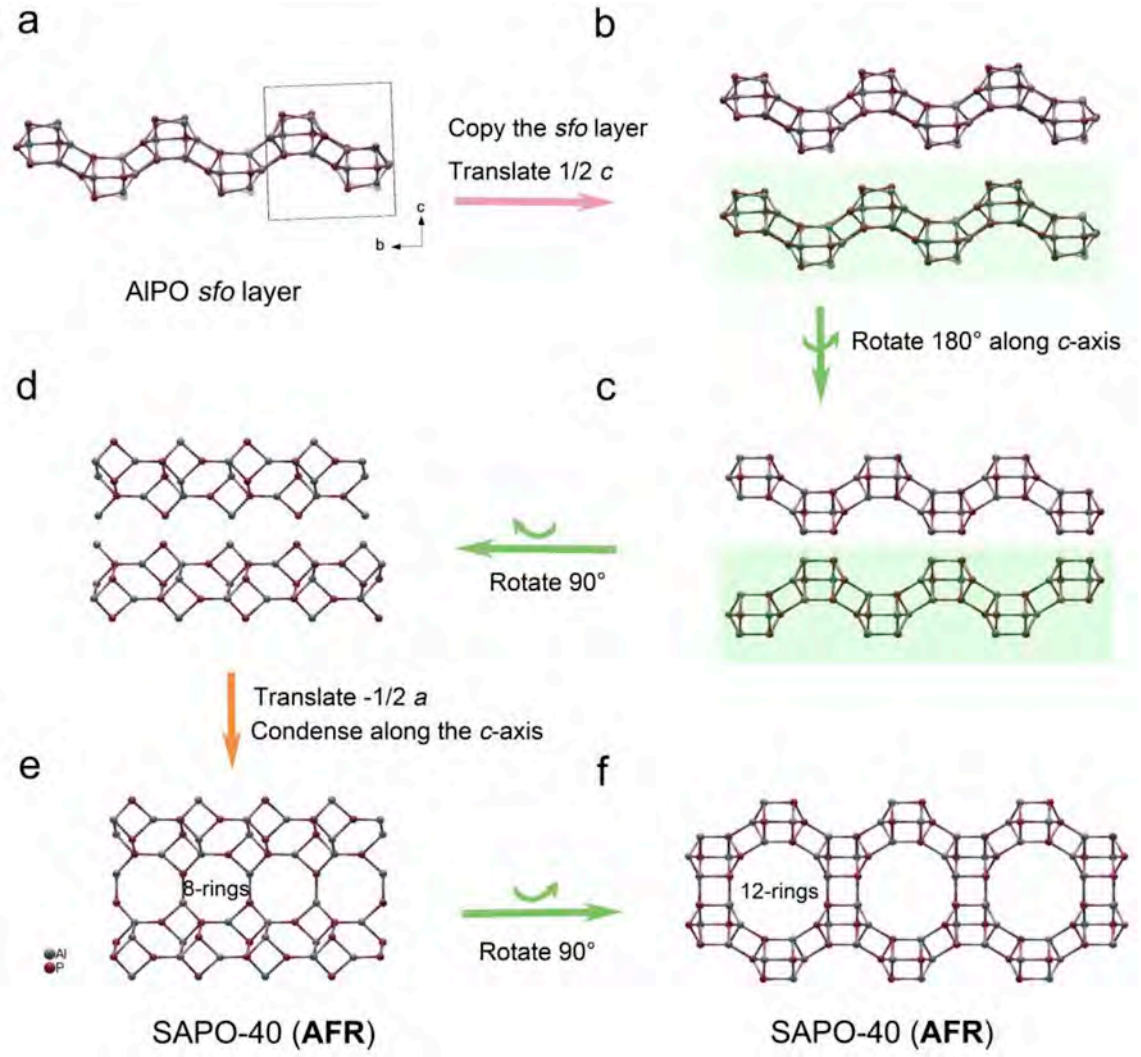

Fig. 13. The **AFR** framework constructed by assembling *afo* layers. The identical AlPO *afo* layer is copied and translated by 1/2 *c* (a and b, highlighted in green). This layer is rotated 180° along *c*-axis (c) with respect to one another, then translated by 1/2 *a*, and condensed along the *c*-axis (d and e) to form the 3D **AFR** framework (e and f). (For interpretation of the references to colour in this figure legend, the reader is referred to the Web version of this article.)

The examples indicate that layered AlPO-based materials can be successfully "organized" and "reassembled" into 3D zeotype frameworks, although the "disassembly" part, the step of forming layered structures, did not come from on-purpose synthetic manipulation of a 3D precursor that should have vulnerable chemical bonds to be further disassembled. Here, we highlight such a possible structure, ECR-40 (**MEI**), which is a 3D SAPO material with a 12x7x7 channel system (Fig. 14a and b) [41–44]. ECR-40 is the only one AlPO-based material that possesses odd-member-ring in its structure. It has been established that the chemical elements Al, P, and Si are distributed orderly and the unusual Al-O-Al bonding in the as-made ECR-40 has been identified from solid-state NMR and Rietveld Refinement.

In the **MEI** framework, the *mei* CBU can be considered as the building block for constructing the 2D undulating AlPO layer within the *ab*-plane, designated as the *mei* layer (Fig. 14c). The *mei* layer and its mirror image are further connected by inserting pure Si 3-rings (Fig. 14b). In this case, the unusual Al-O-Al bonds are simultaneously generated between the AlPO layers. Therefore, the pure Si 3-rings and Al-O-Al bonds are expected to be disassembled through appropriate treatments, resulting in 2D AlPO layers (Fig. 14c) amenable for further organization and reassembly. If the adjacent *mei* layer rotates 60° along the 6_3-screw axis, for example, the Al-OH nests can be identified between the AlPO *mei* layers (Fig. 14d). A SAPO **AFY** framework with a 12x8x8 channel system could be built by inserting one more Si into the Al-OH nest (Fig. 14e and f). As mentioned in the introduction, the SAPO **AFY**-type MS has never been synthesized directly (Fig. S3), therefore, it is tantalizing that the ADOR approach may lead to its synthesis.

5. Conclusions

In this article, we summarize and categorize the AlPO-based MSs. 40 SAPO, 44 AlPO, and 51 MeAPO MSs are identified among the materials deposited in the zeolite database. Several novel (silico)aluminophosphate materials reported in recent years have been highlighted. Then, structural transformations of AlPO-based 2D materials into 3D frameworks have been summarized. Finally, we propose that the ADOR approach pioneered by Prof. Wieslaw J. Roth et al. may be applied to AlPO-based materials. We have identified one potential target: the **AFY**-type SAPO MS starting from SAPO ECR-40. This summary of AlPO-based MSs may provide an inspiration for the synthesis of novel materials with either new frameworks or unprecedented compositions.

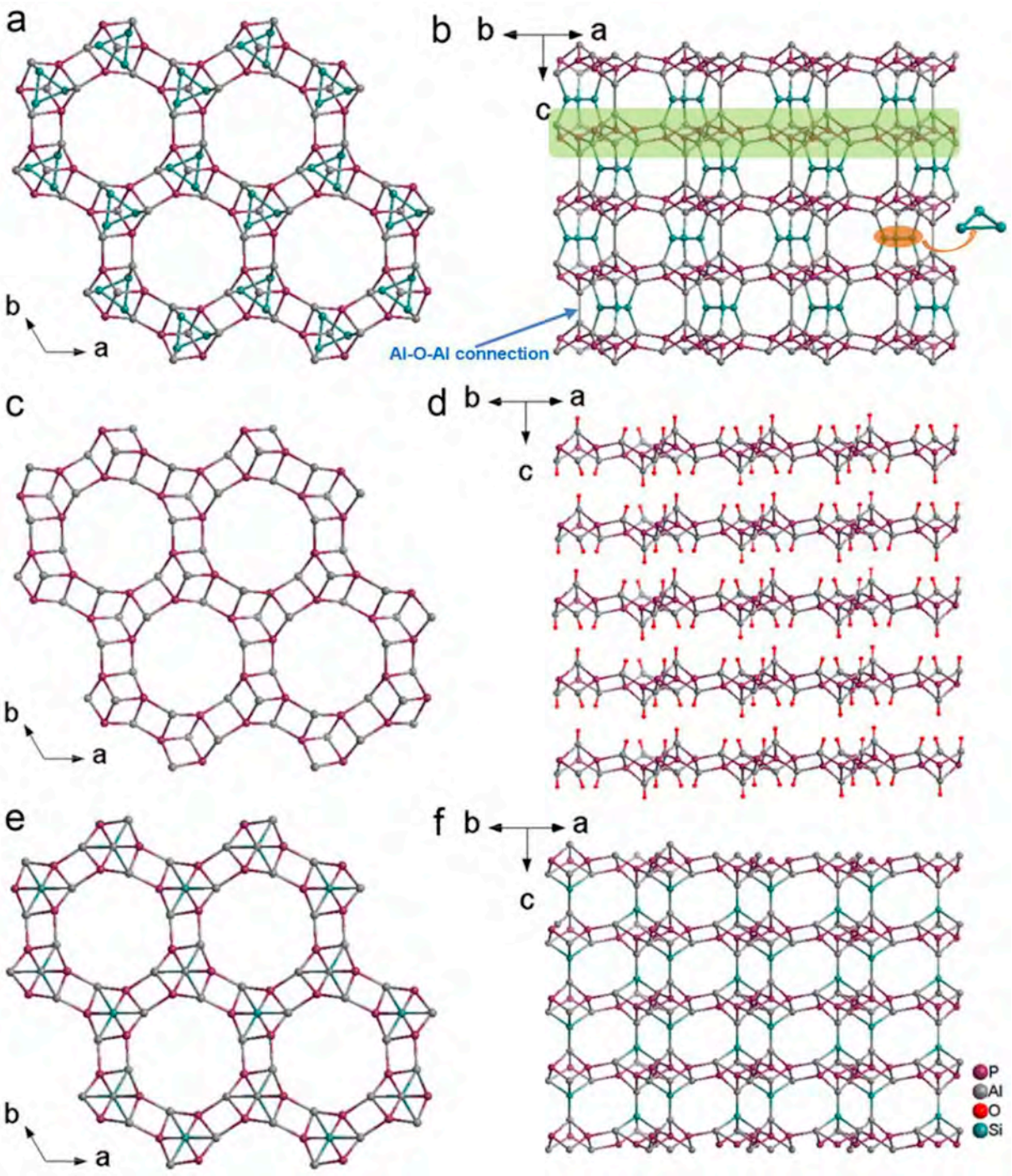

Fig. 14. Structural model of ECR-40 (**MEI**) viewed along the [001] direction (a) and [110] direction (b). Single 3-rings, *mei* layer, and weak Al-O-Al connection are highlighted in the orange ellipse, the green rectangular, and the blue arrow, respectively. *mei* layers (c) viewed along the *c*-axis. The adjacent *mei* layer rotates 60° along the 6_3-screw axis (d). For clarity, O atoms are omitted except for those which are between the separated *mei* layers in Fig. 14d. Structural model of the SAPO form **AFY** framework viewed along the [001] direction (e) and [110] direction (f), respectively. (For interpretation of the references to colour in this figure legend, the reader is referred to the Web version of this article.)

Acknowledgements

Dr. Peng Tian acknowledges financial support from National Natural Science Foundation of China (No. 21676262), Key Research Program of Frontier Sciences, Chinese Academy of Sciences (Grant No. QYZDBSSW-JSC040). Dr. Peng Guo acknowledges financial support from CAS Pioneer Hundred Talents Program (Y706071202). Dr. Lei Wang acknowledges the China Postdoctoral Science Foundation (2018M630308) and DICP Outstanding Postdoctoral Foundation (2017YB07).

Appendix A. Supplementary data

Supplementary data to this article can be found online at https://doi.org/10.1016/j.micromeso.2019.01.047.

References

[1] S.T. Wilson, B.M. Lok, C.A. Messina, T.R. Cannan, E.M. Flanigen, J. Am. Chem. Soc. 104 (1982) 1146–1147, https://doi.org/10.1021/ja00368a062.
[2] P. Tian, Y. Wei, M. Ye, Z. Liu, ACS Catal. 5 (2015) 1922–1938, https://doi.org/10.1021/acscatal.5b00007.
[3] C. Niu, X. Shi, F. Liu, K. Liu, L. Xie, Y. You, H. He, Chem. Eng. J. 294 (2016) 254–263, https://doi.org/10.1016/j.cej.2016.02.086.
[4] S.J. Miller, Microporous Mater. 2 (1994) 439–449, https://doi.org/10.1016/0927-6513(94)00016-6.
[5] S.V. Priya, J.H. Mabel, S. Gopalakrishnan, M. Palanichamy, V. Murugesan, J. Porous Mater. 16 (2009) 419–427, https://doi.org/10.1007/s10934-008-9214-y.
[6] X. Su, P. Tian, D. Fan, Q. Xia, Y. Yang, S. Xu, L. Zhang, Y. Zhang, D. Wang, Z. Liu, ChemSusChem 6 (2013) 911–918, https://doi.org/10.1002/cssc.201200907.
[7] Database of Zeolite Structures, http://www.iza-structure.org/databases/, (Accessed 15, January, 2019).
[8] P. Guo, N. Yan, L. Wang, X. Zou, Cryst. Growth Des. 17 (2017) 6821–6835, https://doi.org/10.1021/acs.cgd.7b01410.
[9] W.J. Roth, P. Nachtigall, R.E. Morris, J. Čejka, Chem. Rev. 114 (2014) 4807–4837, https://doi.org/10.1021/cr400600f.
[10] W.J. Roth, P. Nachtigall, R.E. Morris, P.S. Wheatley, V.R. Seymour, S.E. Ashbrook, P. Chlubná, L. Grajciar, M. Položij, A. Zukal, O. Shvets, J. Čejka, Nat. Chem. 5 (2013) 628–633, https://doi.org/10.1038/nchem.1662.
[11] R.W. Broach, N. Greenlay, P. Jakubczak, L.M. Knight, S.R. Miller, J.P.S. Mowat, J. Stanczyk, G.J. Lewis, Microporous Mesoporous Mater. 189 (2014) 49–63, https://doi.org/10.1016/j.micromeso.2013.09.022.
[12] R. Martinez-Franco, M. Moliner, Y. Yun, J. Sun, W. Wan, X. Zou, A. Corma, Proc. Natl. Acad. Sci. 110 (2013) 3749–3754, https://doi.org/10.1073/pnas.1220733110.
[13] Y. Wang, Y. Li, Y. Yan, J. Xu, B. Guan, Q. Wang, J. Li, J. Yu, Chem. Commun. 49 (2013) 9006–9008, https://doi.org/10.1039/c3cc43375g.
[14] X. Song, Y. Li, L. Gan, Z. Wang, J. Yu, R. Xu, Angew. Chem. Int. Ed. 48 (2009) 314–317, https://doi.org/10.1002/anie.200803578.
[15] Z. Liu, X. Song, J. Li, Y. Li, J. Yu, R. Xu, Inorg. Chem. 51 (2012) 1969–1974, https://doi.org/10.1021/ic2022903.
[16] L. Shao, Y. Li, J. Yu, R. Xu, Inorg. Chem. 51 (2012) 225–229, https://doi.org/10.1021/ic201515z.
[17] S. Seo, T. Yang, J. Shin, D. Jo, X. Zou, S.B. Hong, Angew. Chem. Int. Ed. 57 (2018) 3727–3732, https://doi.org/10.1002/anie.201800791.
[18] J.K. Lee, A. Turrina, L. Zhu, S. Seo, D. Zhang, P.A. Cox, P.A. Wright, S. Qiu, S.B. Hong, Angew. Chem. Int. Ed. 53 (2014) 7480–7483, https://doi.org/10.1002/anie.201402495.
[19] Z. Han, A.L. Picone, A.M.Z. Slawin, V.R. Seymour, S.E. Ashbrook, W. Zhou, S.P. Thompson, J.E. Parker, P.A. Wright, Chem. Mater. 22 (2010) 338–346, https://doi.org/10.1021/cm902528y.
[20] A. Turrina, R. Garcia, A.E. Watts, H.F. Greer, J. Bradley, W. Zhou, P.A. Cox, M.D. Shannon, A. Mayoral, J.L. Casci, P.A. Wright, Chem. Mater. 29 (2017) 2180–2190, https://doi.org/10.1021/acs.chemmater.6b04892.
[21] S. Liang, Y. Zhang, Y. Wan, X. Mu, G. Xu, X. Shu, CN 108147423A.
[22] Y. Wei, Z. Tian, H. Gies, R. Xu, H. Ma, R. Pei, W. Zhang, Y. Xu, L. Wang, K. Li, B. Wang, G. Wen, L. Lin, Angew. Chem. Int. Ed. 49 (2010) 5367–5370, https://doi.org/10.1002/anie.201000320.
[23] S.H. Park, W. Choi, H.J. Choi, S.B. Hong, Angew. Chem. Int. Ed. 57 (2018) 9413–9418, https://doi.org/10.1002/anie.201805089.
[24] A. Turrina, R. Garcia, P.A. Cox, J.L. Casci, P.A. Wright, Chem. Mater. 28 (2016) 4998–5012, https://doi.org/10.1021/acs.chemmater.6b01676.
[25] M. Castro, R. Garcia, S.J. Warrender, A.M.Z. Slawin, P.A. Wright, P.A. Cox, A. Fecant, C. Mellot-Draznieks, N. Bats, Chem. Commun. (2007) 3470–3472, https://doi.org/10.1039/b705377k.
[26] Y. Umehara, M. Itakura, N. Yamanaka, M. Sadakane, T. Sano, Microporous Mesoporous Mater. 179 (2013) 224–230, https://doi.org/10.1016/j.micromeso.2013.06.013.
[27] X. Su, P. Tian, J. Li, Y. Zhang, S. Meng, Y. He, D. Fan, Z. Liu, Microporous Mesoporous Mater. 144 (2011) 113–119, https://doi.org/10.1016/j.micromeso.2011.04.004.
[28] R. Martinez-Franco, J. Sun, G. Sastre, Y. Yun, X. Zou, M. Moliner, A. Corma, Proc. R. Soc. A. 470 (2014) 20140107, https://doi.org/10.1098/rspa.2014.0107.
[29] D. Xie, L.B. McCusker, C. Baerlocher, S.I. Zones, W. Wan, X. Zou, J. Am. Chem. Soc. 135 (2013) 10519–10524, https://doi.org/10.1021/ja4043615.
[30] N. Yan, L. Wang, X. Liu, P. Wu, T. Sun, S. Xu, J. Han, P. Guo, P. Tian, Z. Liu, J. Mater. Chem. 6 (2018) 24186–24193, https://doi.org/10.1039/c8ta08134d.
[31] P.S. Wheatley, C.J. Love, J.J. Morrison, I.J. Shannon, R.E. Morris, J. Mater. Chem. 12 (2002) 477–482, https://doi.org/10.1039/b106005h.
[32] P.S. Wheatley, R.E. Morris, J. Mater. Chem. 16 (2006) 1035–1037, https://doi.org/10.1039/b518265d.
[33] P. Guo, M. Afeworki, G. Cao, Y. Yun, J. Sun, J. Su, W. Wan, X. Zou, Inorg. Chem. 57 (2018) 11753–11760, https://doi.org/10.1021/acs.inorgchem.8b01890.
[34] G. Cao, M. Afeworki, G.J. Kennedy, K.G. Strohmaier, D.L. Dorset, Acta Cryst. B63 (2007) 56–62, https://doi.org/10.1107/S0108768106040109.
[35] R.E. Morris, A. Burton, L.M. Bull, S.I. Zones, Chem. Mater. 16 (2004) 2844–2851, https://doi.org/10.1021/cm0353005.
[36] M.A. Estermann, L.B. McCusker, C. Baerlocher, J. Appl. Cryst. 25 (1992) 539–543, https://doi.org/10.1107/S0021889892004862.
[37] L.B. McCusker, C. Baerlocher, Microporous Mater. 6 (1996) 51–54, https://doi.org/10.1016/0927-6513(95)00078-X.
[38] P. Eliášová, M. Opanasenko, P.S. Wheatley, M. Shamzhy, M. Mazur, P. Nachtigall, W.J. Roth, R.E. Morris, J. Čejka, Chem. Soc. Rev. 44 (2015) 7177–7206, https://doi.org/10.1039/C5CS00045A.
[39] J.-L. Paillaud, B. Harbuzaru, J. Patarin, N. Bats, Science 304 (2004) 990–992, https://doi.org/10.1126/science.1098242.
[40] M. Mazur, P.S. Wheatley, M. Navarro, W.J. Roth, M. Položij, A. Mayoral, P. Eliášová, P. Nachtigall, J. Čejka, R.E. Morris, Nat. Chem. 8 (2016) 58–62, https://doi.org/10.1038/nchem.2374.
[41] D. E. W. Vaughan, F. J.N, US Patent 5976491.
[42] A. M, D.L. Dorset, G.J. Kennedy, K.G. Strohmaier, E. van Steen, L.H. Callanan, M. Claeys (Eds.), Studies in Surface Science and Catalysis, Elsevier, 2004, pp. 1274–1281, , https://doi.org/10.1016/S0167-2991(04)80639-6.
[43] J.K. Lee, J.H. Lee, N.H. Ahn, K.H. Cho, S.B. Hong, Chem. Sci. 7 (2016) 5805–5814, https://doi.org/10.1039/C6SC02092E.
[44] J.K. Lee, J. Shin, N.H. Ahn, A. Turrina, M.B. Park, Y. Byun, S.J. Cho, P.A. Wright, S.B. Hong, Angew. Chem. Int. Ed. 54 (2015) 11097–11101, https://doi.org/10.1002/anie.201504416.